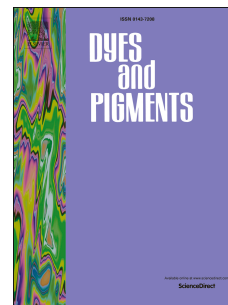


Accepted Manuscript

New sky-blue and bluish-green emitting Ir(III) complexes containing an azoline ancillary ligand for highly efficient PhOLEDs

Ganguri Sarada, Bomi Sim, Woosum Cho, Juho Yoon, Yeong-Soon Gal, Jang-Joo Kim, Sung-Ho Jin



PII: S0143-7208(16)30121-8

DOI: [10.1016/j.dyepig.2016.03.053](https://doi.org/10.1016/j.dyepig.2016.03.053)

Reference: DYPI 5178

To appear in: *Dyes and Pigments*

Received Date: 23 February 2016

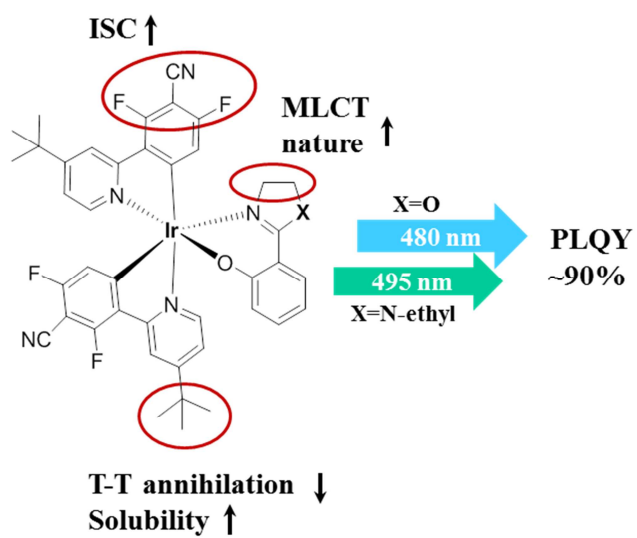
Revised Date: 30 March 2016

Accepted Date: 31 March 2016

Please cite this article as: Sarada G, Sim B, Cho W, Yoon J, Gal Y-S, Kim J-J, Jin S-H, New sky-blue and bluish-green emitting Ir(III) complexes containing an azoline ancillary ligand for highly efficient PhOLEDs, *Dyes and Pigments* (2016), doi: 10.1016/j.dyepig.2016.03.053.

This is a PDF file of an unedited manuscript that has been accepted for publication. As a service to our customers we are providing this early version of the manuscript. The manuscript will undergo copyediting, typesetting, and review of the resulting proof before it is published in its final form. Please note that during the production process errors may be discovered which could affect the content, and all legal disclaimers that apply to the journal pertain.

Graphical Abstract



New Sky-blue and Bluish-green Emitting Ir(III) Complexes Containing an Azoline Ancillary Ligand for Highly Efficient PhOLEDs

Ganguri Sarada,^a Bomi Sim,^c Woosum Cho,^a Juho Yoon,^a Yeong-Soon Gal,^b Jang-Joo Kim,^{*c} and Sung-Ho Jin^{*a}

^a Department of Chemistry Education, Graduate Department of Chemical Materials, and Institute for Plastic Information and Energy Materials, Pusan National University, Busan, 609-735, Republic of Korea, E-mail: shjin@pusan.ac.kr

^b Polymer Chemistry Laboratory, College of Engineering, Kyungil University, Gyeongsan 712-701, Republic of Korea.

^c Department of Materials Science and Engineering, Seoul National University, Seoul 151-744, Republic of Korea, E-mail: jjkim@snu.ac.kr

† Electronic supplementary information (ESI) available.

Abstract: Two Ir(III) complexes containing the chromophoric ancillary ligands 2-(4,5-dihydrooxazol-2-yl)phenol and 2-(1-ethyl-4,5-dihydro-1*H*-imidazol-2-yl)phenol, and a highly functionalized phenylpyridine derivative, 3-(4-(*tert*-butyl)pyridin-2-yl)-2,6-difluorobenzonitrile, as a cyclometalating ligand were designed and synthesized. The oxazoline/imidazoline heterocycle of the ancillary ligand has the effect of enhancing the metal to ligand charge transfer transition nature of the emitting excited state and the fluorine and cyano substituents on the ligand have enriched the intersystem crossings, as indicated by the experimental photoluminescence analysis. As a result, the oxazoline and imidazoline containing complexes exhibited high photoluminescence quantum yields of about >90% with bright sky-blue emission at 480 nm and bluish-green light at 495 nm, respectively, along with excellent thermal/morphological stability about 400 °C and good solubility, that make them suitable for both wet- and dry-processes. In particular, the phosphorescent OLEDs fabricated by a dry-process showed the maximum EQEs of 21.9% and 19.7% for the oxazoline and imidazoline containing complexes, respectively.

Keywords: phosphorescent organic light-emitting diode; iridium complex; rigidity; intersystem crossings; photoluminescence quantum yields; external quantum efficiency

1. Introduction

Organic light-emitting diodes (OLEDs) are one of the most successful devices in the field of organic electronics with rapid commercialization in both display and lighting applications [1,2]. Phosphorescent materials play a key role as emitters for fabrication of highly efficient OLEDs as they can harvest both singlet (S_1) and triplet (T_1) excitons through strong spin-orbit coupling (SOC) assisted intersystem crossings (ISC) [3]. Among the heavy metal complexes, neutral iridium(III) complexes are the most famous phosphors for application in phosphorescent OLEDs (PhOLEDs) because of their high color tunability, short excited-state lifetime and thermal stability [4-6]. In addition, Ir(III) complexes must possess high photoluminescence quantum yields (PLQYs) for attaining high performance PhOLEDs.

Heteroleptic Ir(III) complexes are synthetically easier to access than the homoleptic counterparts, though the latter are more stable due to their rigidity. Chromophoric ancillary ligands are a new class of ligands that are anticipated to yield high PLQYs compared with the non-chromophoric ones because the Ir(III) complexes with chromophoric ancillary ligands can harvest more energy by excitation of both the ancillary ligand and the cyclometalating ($C^{\wedge}N$) ligand [7]. Furthermore, Ir(III) complexes with these type of ancillary ligands are expected to have high rigidity and thermal stability thus being comparable with the homoleptic analogs. However, very limited research was carried out so far on this class of Ir(III) complexes [8-10]. An exemplary type of chromophoric ligand; 2-(2-hydroxyphenyl) benzazole has good electron accepting nature, therefore, is widely used in Al(III), Be(II), and Zn(II) complexes to obtain efficient electron transporting materials, host materials and emitters for OLED applications [11-17]. A comprehensive experimental and theoretical study by S. Y. Park et al. on a series of Ir(III) complexes containing 2-(2-hydroxyphenyl)oxazole based chromophoric ancillary ligands and a

difluorophenylpyridine (dfppy) based C^N ligand revealed that emission originates from the ancillary ligand centered ³L_AC state by an interligand energy transfer (ILET) from C^N ligand to the ancillary ligand exhibiting a weak interaction with MLCT [8]. Conversely, a large contribution of MLCT in the emitting (lowest) excited state is very important to achieve high radiative relaxation and PLQYs [18-24]. Z. Wu et al. have carried out computational studies on a series of Ir(III) complexes containing 2-hydroxyphenyl attached oxazoline or imidazoline based ancillary ligands and phenylpyridine (ppy) as C^N ligand [10]. Their study elucidates that these Ir(III) complexes possess a large contribution of MLCT in the emitting excited state and a small S₁-T₁ splitting energy ($\Delta E_{S_1-T_1}$), unlike the previous study, and are thus, proposed to have higher PLQYs than the other complexes with less MLCT contribution.

We anticipate that replacement of oxazole with oxazoline would enhance the MLCT contribution in the Ir(III) complexes by raising ³L_AC energy level close to MLCT level due to the reduced conjugation in the heterocycle, yet maintains the advantages of the chromophoric ancillary ligands. Based on this, we designed and synthesized two Ir(III) complexes with 2-(4,5-dihydrooxazol-2-yl)phenol (**oz**) and 2-(1-ethyl-4,5-dihydro-1*H*-imidazol-2-yl)phenol (**im**) as ancillary ligands and the ppy scaffold that was highly derivatized with electron-withdrawing (-F and -CN) and electron-donating (*tert*-butyl) groups as C^N ligand, and well-studied their photophysical process.

The new Ir(III) complexes possess high PLQYs, good solubility in common organic solvents, and high thermal and morphological stabilities making them suitable for solution-process as well as vapor deposition techniques for further commercialization purposes. We fabricated monochromatic PhOLEDs by both solution-process and vapor deposition methods by employing the new Ir(III) complexes as dopants and achieved the high external quantum

efficiency (EQE) of 21.9% for the sky-blue emitting oz-based complex (**tBuCN-FIroz**) and 19.7% for the bluish-green emitting im-based complex (**tBuCN-FIrim**) in vapor deposition method.

2. Experimental Section

Synthesis of 2-(4,5-dihydrooxazol-2-yl)phenol (oz). Methyl 2-hydroxybenzoate (**1**) (44 g, 0.29 mol) and ethanolamine (18.4 g, 0.29 mol, 18 mL) were reacted at 150 °C for 2 h. During the reaction, methanol was evolved and which was collected in a Dean–Stark trap. A red-brown viscous liquid was obtained and it was trituration in benzene to yield a pink solid. A white crystals of N-(2-hydroxyethyl)-2-hydroxybenzamide (**2**) (27 g, 52%) were obtained after recrystallization in ethyl acetate. To a solution of **2** (27 g, 0.15 mol) in chloroform (300 mL), thionyl chloride (59 g, 0.5 mol) was added dropwise at 0 °C and the reaction was carried out overnight at room temperature. The precipitated pink solid was filtered off, washed several times with chloroform, and dried under vacuum. To the intermediate 2-(2-hydroxyphenyl)-2-oxazolinium chloride (21 g, 71%) and water (200 mL), saturated aqueous NaHCO₃ was added. The precipitated solid was isolated (14 g). Color: Light pink solid. Yield: 81%. M.P.: 39 °C. IR data (KBr) cm⁻¹: 3074, 2990, 2953, 2885, 1641, 1493, 1371, 1252, 1231, 1152, 1127, 1067, 940, 800. ¹H NMR (300 MHz, CD₃OD, δ): 7.64-7.62 (d, J=7.8 Hz, 1H, Ar-H), 7.38-7.33 (t, J=15.3 Hz, 1H, Ar-H), 6.93-6.90 (d, J=8.4 Hz, 1H, Ar-H), 6.88-6.83 (t, J=14.7 Hz, 1H, Ar-H), 4.45-4.39 (t, J=18.6 Hz, 2H, Oz-CH₂), 4.08-4.02 (t, J=18.6 Hz, 2H, Oz-CH₂). ¹³C NMR (75 MHz, CD₃OD, δ): 165.91, 159.46, 132.90, 127.68, 118.30, 116.00, 110.506, 66.65, 52.94. Anal. Calcd for C₉H₉NO₂: C, 66.25; H, 5.56; N, 8.58. Found C, 65.89; H, 5.77; N, 8.82. UV-Vis: λ_{max} (CHCl₃):

305 nm. Fluorescence: excitation λ_{\max} : 305 nm, emission λ_{\max} (CHCl₃): 460 nm, stokes shift: 155 nm.

Synthesis of 2-(1-ethyl-4,5-dihydro-1H-imidazol-2-yl)phenol (im). A mixture of Methyl 2-hydroxybenzoate (**1**) (2 g, 13.1 mmol) and *N*-Ethyl ethylenediamine (3.48 g, 39.5 mmol) was refluxed overnight. The unreacted *N*-Ethyl ethylenediamine was evaporated off under vacuum. A yellow viscous gel was obtained after cooling the residue to room temperature. It was triturated in a small amount of hexane to yield white solid, which was further purified by crystallization in methanol to obtain pure product (1.15 g). Color: White solid. Yield: 46%. M.P.: 130 °C. IR data (KBr) cm⁻¹: 3239, 3049, 2980, 2938, 2696, 2480, 1630, 1538, 1456, 1440, 1302, 1238, 1190, 1139, 872, 765, 687. ¹H NMR (300 MHz, CD₃OD, δ): 7.78-7.75 (d, J=8.1 Hz, 1H, Ar-H), 7.30-7.25 (t, J=13.5 Hz, 1H, Ar-H), 6.83-6.80 (d, J=8.1 Hz, 1H, Ar-H), 6.74-6.69 (t, J=14.7 Hz, 1H, Ar-H), 3.61-3.57 (t, J=11.7 Hz, 2H, Im-CH₂), 2.97-2.93 (t, J=11.7 Hz, 2H, Im-CH₂), 2.85-2.78 (m, 2H, N-CH₂), 1.21-1.16 (t, J=14.7 Hz, 3H, N-CH₂CH₃). ¹³C NMR (75 MHz, CD₃OD, δ): 170.57, 163.52, 133.15, 128.14, 118.92, 116.53, 116.42, 47.03, 42.97, 37.30, 12.12. Anal. Calcd for C₁₁H₁₄N₂O: C, 69.45; H, 7.42; N, 14.73. Found C, 69.83; H, 7.68; N, 14.29. UV-Vis: λ_{\max} (CHCl₃): 306 nm. Fluorescence: excitation λ_{\max} : 305 nm, emission λ_{\max} (CHCl₃): 439 nm, stokes shift: 133 nm.

General procedure for synthesis of the Ir(III) complexes. To a solution of dimer (**3**) (0.9 g, 0.58 mmol) in 1,4-dioxane (30 mL), the ancillary ligand (**oz**) (0.95 g, 5.8 mmol) and anhydrous K₂CO₃ (0.405 g, 2.9 mmol) were added and refluxed for 6 h at 105 °C under N₂ atmosphere. HCl (1N, 10 mL) was added to the reaction mixture and extracted with CH₂Cl₂. Organic layer was dried over anhydrous Na₂SO₄ and concentrated under vacuum. The crude product was purified by column chromatography on silica gel (EtOAc:Hexane, 3:7 v/v) to obtain the final compound.

Bis{3-[4-(*tert*-butyl)pyridin-2-yl]-2,6-difluorobenzonitrile}(2-(4,5-dihydrooxazol-2-yl)phenolate)iridium(III) [tBuCN-FIroz]. Color: Yellow powder. Yield: 50%. M.P.: not detected up to 390 °C. IR data (KBr) cm^{-1} : 2962, 2231, 1612, 1535, 1470, 1441, 1410, 1351, 1295, 1235, 1035, 851. ^1H NMR (300 MHz, CDCl_3 , δ): 8.64-8.62 (d, $J=6$ Hz, 1H, Ar-H), 8.32-8.29 (d, $J=8.1$ Hz, 2H, Ar-H), 8.20-8.18 (d, 1H, $J=6$ Hz, Ar-H), 7.64-7.62 (d, $J=7.8$ Hz, 1H, Ar-H), 7.34-7.32 (d, $J=4.2$ Hz, 1H, Ar-H), 7.24-7.22 (d, $J=6$ Hz, 1H, Ar-H), 7.19-7.16 (d, $J=8.7$ Hz, 1H, Ar-H), 6.71-6.68 (d, $J=8.1$ Hz, 1H, Ar-H), 6.46-6.41 (t, $J=14.1$ Hz, 1H, Ar-H), 5.94-5.92 (d, $J=8.1$ Hz, 1H, Ar-H), 5.74-5.71 (d, $J=8.7$ Hz, 1H, Ar-H), 4.42-4.27 (m, 2H, Oz- CH_2), 3.62-3.52 (m, 1H, Oz-CH), 3.13-3.03 (q, 1H, Oz-CH), 1.45-1.42 (d, $J=10.2$ Hz, 18H, tBu). ^{13}C NMR (75 MHz, CDCl_3 , δ): 168.45, 167.39, 164.56, 163.90, 163.67, 163.38, 162.42, 161.96, 161.64, 160.32, 157.96, 148.45, 147.82, 134.03, 130.04, 129.87, 129.56, 124.89, 121.21, 120.94, 120.31, 120.06, 116.14, 115.94, 115.31, 115.08, 113.77, 111.12, 110.96, 109.31, 66.57, 54.82, 35.38, 30.57. Anal. Calcd for $\text{C}_{41}\text{H}_{34}\text{F}_4\text{IrN}_5\text{O}_2$: C, 54.90; H, 3.82; N, 7.91. Found C, 54.73; H, 3.91; N, 7.76. UV-Vis: λ_{max} (CHCl_3): 280 nm. Photoluminescence: excitation λ_{max} : 373 nm, emission λ_{max} (CHCl_3): 480 nm, stokes shift: 200 nm. X-ray crystallographic data: Triclinic, CCDC 1423073.

Bis{3-[4-(*tert*-butyl)pyridin-2-yl]-2,6-difluorobenzonitrile}(2-(1-ethyl-4,5-dihydro-1H-imidazol-2-yl)phenolate)iridium(III) [tBuCN-FIrim]. Color: Yellow powder. Yield: 35%. M.P.: 334 °C (decomp.). IR data (KBr) cm^{-1} : 2968, 2231, 1605, 1571, 1538, 1483, 1470, 1435, 1423, 1410, 1333, 1290, 1251, 1033, 848. ^1H NMR (300 MHz, CDCl_3 , δ): 9.02-9.0 (d, $J=5.7$ Hz, 1H, Ar-H), 8.34 (s, 1H, Ar-H), 8.08 (s, 1H, Ar-H), 8.05-8.03 (d, $J=6.3$ Hz, 1H, Ar-H), 7.37-7.35 (d, $J=5.7$ Hz, 1H, Ar-H), 7.07-7.04 (d, $J=9$ Hz, 1H, Ar-H), 6.82 (m, 2H, Ar-H), 6.42-6.37 (t, $J=14.7$ Hz, 1H, Ar-H), 6.26-6.23 (d, $J=8.7$ Hz, 1H, Ar-H), 6.17-6.15 (d, $J=8.7$ Hz, 1H, Ar-H),

5.66-5.63 (d, $J=9$ Hz, 1H, Ar-H), 3.76-3.66 (m, 2H, Im-CH₂), 3.20-3.11 (m, 1H, Im-CH), 3.04-2.92 (m, 2H, N-CH₂), 2.76-2.65 (m, 1H, Im-CH), 1.49 (s, 9H, tBu), 1.32 (s, 9H, tBu), 1.24-1.17 (t, $J=15$ Hz, 3H, N-CH₂CH₃). ¹³C NMR (75 MHz, CDCl₃, δ): 171.10, 168.50, 166.26, 163.98, 163.61, 162.83, 149.49, 148.52, 132.52, 130.02, 129.81, 128.41, 123.43, 120.48, 120.16, 119.82, 119.56, 119.34, 116.56, 116.34, 116.20, 115.48, 115.28, 114.12, 111.48, 50.79, 49.60, 46.12, 35.57, 35.22, 30.76, 30.45, 14.18. Anal. Calcd for C₄₃H₃₉F₄IrN₆O: C, 55.89; H, 4.25; N, 9.06. Found C, 55.70; H, 4.19; N, 9.19. UV-Vis: λ_{max} (CHCl₃): 281 nm. Photoluminescence: excitation λ_{max} : 373 nm, emission λ_{max} (CHCl₃): 495 nm, stokes shift: 213 nm. X-ray crystallographic data: Monoclinic, CCDC 1423074.

3. Results and Discussion

3.1 Synthesis and Characterization

The detailed synthetic route and the chemical structures of the new Ir(III) complexes: **tBuCN-FIroz** and **tBuCN-FIrim** are given in Scheme 1. Ancillary ligand **oz** and the dimer (**3**) were synthesized as per the reported procedures [25,26]. The ancillary ligand **im** was synthesized as per the modified procedure [27]. The new Ir(III) complexes were well characterized by ¹H, ¹³C NMR (Fig. S1-S4, ESI⁺), IR spectra (Fig. S5, ESI⁺) and single crystal XRD for structural confirmation (Table S1 & S2, ESI⁺).

3.2. Single Crystal XRD Characterizations

tBuCN-FIroz (CCDC 1423073) and **tBuCN-FIrim** (CCDC 1423074) possess distorted octahedral geometry around the iridium center with the two C^N ligands positioned *N,N*-trans and *C,C*-cis pattern (Fig. 1). As shown in Fig. S6 (ESI⁺), molecules of **tBuCN-FIroz** pack with a few intermolecular contacts (2.93 and 2.84 Å) by C-H \cdots π interactions, whereas those of

tBuCN-FIrim pack with several intermolecular contacts and relatively stronger C-H \cdots F interactions (2.64, 2.87 Å and 2.7, 2.84 Å). The ancillary ligand of **tBuCN-FIrim** is configurationally distorted with torsion angles of -31.71° [N5-C39-C38-C33] and -30.37° [N6-C39-C38-C37] due to the presence of alkyl group. Such distortion is not observed in the case of **tBuCN-FIroz** as from the torsion angles 4.72° [C9-C4-C3-N1] and 2.52° [C5-C4-C3-O1] indication its rigid nature.

3.3. Thermal Properties

Thermal stabilities of the Ir(III) complexes were evaluated by measuring the decomposition (T_d , at 5% weight loss) and the glass transition (T_g) temperatures using thermogravimetric analysis (TGA) and derivative thermogravimetric analysis (DTA), respectively. Unlike that of the already reported heteroleptic Ir(III) complexes with conventional ancillary ligands such as acetylacetonate and picolinate, T_d of **tBuCN-FIroz** and **tBuCN-FIrim** is very high about 423 and 403 °C (Fig. 2a), respectively, and T_g was not observed within 300 °C (see Fig. 2b & c). Thermal stability of **tBuCN-FIroz** is higher than **tBuCN-FIrim** due to the high rigidity of the ancillary ligand, **oz**. The high thermal and morphological stabilities of **tBuCN-FIroz** and **tBuCN-FIrim** render them suitable for both thermal evaporation and solution-process with annealing treatments.

3.4. Photophysical Properties

UV-visible absorption and the photoluminescence (PL) spectra of **tBuCN-FIroz** and **tBuCN-FIrim** measured in CHCl₃ (10⁻⁵ M) at room temperature are given in Fig. 3a. **tBuCN-FIroz** emits bright sky-blue light at the maximum PL (PL_{max}) intensity of 480 nm and **tBuCN-FIrim** emits bluish-green light at PL_{max} of 495 nm in a structureless manner with a single peak indicating MLCT contribution in the emitting excited state [28]. Furthermore, **tBuCN-FIroz** and

tBuCN-FIrim demonstrated positive solvatochromism (Fig. S7, ESI†) with a variation in PL_{max} of about 21-24 nm depending on the solvent polarity supporting the charge transfer nature of the emission [29,30]. In contrast, the emission pattern of **tBuCN-FIroz** and **tBuCN-FIrim** resembles the emission of their respective ancillary ligands as shown in Fig. 3b. This indicates that emission from these Ir(III) complexes originates from the ancillary ligand centred excited state. As shown in Fig. 3c & d, overlap of the PL spectrum of the free C^N ligand with the UV spectra of the ancillary ligands supports the energy transfer from C^N ligand to the ancillary ligand, while the reverse has not occurred. In order to understand the detailed mechanism of the photophysical process, we calculated the excited state S_1 & T_1 energy levels of **tBuCN-FIroz** and **tBuCN-FIrim** from the RT and low temperature PL analysis (Fig. 4).

The schematic energy level diagram, given in Fig. 5, illustrates the possibility of ILET from the C^N ligand centred- 3ML_CCT or $^3L_C C$ state to the ancillary ligand centred- $^3L_A C$ state because of the higher energy of C^N ligand centred state. This indicates that emission of **tBuCN-FIroz** and **tBuCN-FIrim** originates from $^3L_A C$ state. However, the lowest excited state ($^3L_A C$) energy level of **tBuCN-FIroz** (2.66 eV) and **tBuCN-FIrim** (2.58 eV) is elevated relative to the reported Ir(III) complex with oxazole-based ancillary ligand (complex **1**, 2.48 eV) [8], this gets $^3L_A C$ level closer to the $^3ML_CCT/{}^3L_C C$ and 1ML_CCT states (Fig. 5) indicating the possibility of MLCT contribution in the lowest excited state, which is very important for achieving high PLQYs. This MLCT contribution is further strengthened by the theoretical calculations of Z. Wu et al. on Ir(III) complexes with the similar ancillary ligands [10]. In addition, the substituents (-F and -CN) on the C^N ligand are expected to increase the ISC rates, which is very essential to improve the internal quantum efficiency (IQE) of the Ir(III) complexes. As a matter of fact, the C^N ligand showed significant phosphorescence even in dilute solutions at low temperature (see

Fig. 4g) as a representation of strong SOC. In conclusion, this type of energy harvesting process by both the C^N ligand and the chromophoric ancillary ligand along with the enhanced ISC and MLCT nature are advantageous to obtain bright emissions with high PLQYs.

Emission from the neat films of **tBuCN-FIroz** and **tBuCN-FIrim** is red shifted by about 19-22 nm in comparison with the PL_{max} in solution, which is rational considering the strong solid-state interactions described in XRD section. As anticipated, **tBuCN-FIroz** and **tBuCN-FIrim** have exhibited high absolute PLQYs of 90±3% and 89±3%, respectively. The horizontal dipole orientations (Θ) measured for **tBuCN-FIroz** and **tBuCN-FIrim** as a thin films of pBCb2Cz:TSPO1:10% Ir(III) complex are 0.78 and 0.73, respectively (Fig. S8, ESI[†]). A high Θ value of the emitter enhances the light out-coupling efficiency of the PhOLEDs [26,31].

3.5. Electrochemical and DFT Calculations

Highest occupied molecular orbital (HOMO) energy levels of **tBuCN-FIroz** and **tBuCN-FIrim** were calculated from the oxidation peak potentials obtained from cyclic voltammetry (CV) analysis (Fig. S9, ESI[†]). Optical band gaps (E_g) were calculated from the UV-absorption edge and subsequently the lowest occupied molecular orbital (LUMO) energy levels were calculated from the HOMO and E_g (see the data in Table 1). The HOMO energy levels calculated using density functional theory (DFT) are -5.29 and -5.18 eV for **tBuCN-FIroz** and **tBuCN-FIrim**, respectively, agree with the experimental values. From the DFT analysis (Fig. 6), HOMO is distributed on phenolate part of the ancillary ligand and iridium metal centre; whereas LUMO is located mostly on one of the C^N ligands as common for both the Ir(III) complexes, and slightly on oxazoline ring for **tBuCN-FIroz** and on imidazoline ring for **tBuCN-FIrim**, which is well matched with the reported analogous molecules [9]. Permanent dipole moment (μ) of **tBuCN-FIroz** is 12.04D and **tBuCN-FIrim** is 13.23D, obtained from DFT analysis. The slight increase

in μ for **tBuCN-FIrim** is the reason for its close packing in the solid-state with the shortest intermolecular separation (Fig. S6) [31], consequently PL_{\max} of **tBuCN-FIrim** is red shifted relative to **tBuCN-FIroz**.

3.6. Sky-blue and Bluish-green Emitting PhOLEDs

3.6.1. PhOLEDs via Vapor Deposition

The optimized PhOLEDs, where **tBuCN-FIroz** (device A) and **tBuCN-FIrim** (device B) were used as dopants, have the configuration of indium tin oxide (ITO) (70 nm)/ReO₃ (1 nm)/pBCb2Cz (40 nm)/pBCb2Cz:TSPO1:10 wt% Ir(III) complex (30 nm)/TSPO1 (35 nm)/Al (100 nm). Here, 9-(4-(9*H*-pyrido[2,3-*b*]indol-9-yl)phenyl)-9*H*-3,9'-bicarbazole (pBCb2Cz) was used as hole transporting layer (HTL), diphenylphosphine oxide-4-(triphenylsilyl)phenyl (TSPO1) as electron transporting layer (ETL) and pBCb2Cz:TSPO1:Ir(III) complex as emitting layer (EML). The hosts were selected to have higher T_1 energy levels (pBCb2Cz ($T_1=2.93$ eV) and TSPO1 ($T_1=3.4$ eV)) than the two Ir(III) complexes ($T_1<2.7$ eV).

The current density-voltage-luminance (J-V-L) and the EQE-L characteristics of the PhOLEDs are given in Fig. 7a and b. As the HOMO-LUMO energy levels of both the Ir(III) complexes are close to each other, J-V characteristics of the corresponding devices have similar trends with the same turn-on voltage (V_{on}) of 3.3 V and current densities. The maximum EQEs of the PhOLEDs with **tBuCN-FIroz** and **tBuCN-FIrim** are 21.9% and 19.7%, and the EQEs at 1000 cd m⁻² are 20.1% and 17.4%, respectively. This high efficiency of the **tBuCN-FIroz** based device is mainly due to the high PLQY and Θ of the emitter in the thermally deposited films. The electroluminescence (EL) spectrum of the **tBuCN-FIroz** based device is almost the same as the PL spectrum in solution resulting in the sky-blue CIE coordinates (0.149, 0.349), whereas the bluish-green coordinates (0.214, 0.504) were observed for the **tBuCN-FIrim** based device at 10

mA cm^{-2} (Fig. 7c & d). These color coordinates are unchanged throughout the measured current densities.

3.6.2. PhOLEDs via Solution Process

We fabricated solution-processed PhOLEDs driven by the excellent solubility and morphological stability of the two Ir(III) complexes. The two optimized PhOLEDs have the following configuration; ITO/GraHIL (40 nm)/TCTA:DCzPPy:Ir(III) complex (10 wt%, 40 nm)/TPBi (30 nm)/LiF (1 nm)/Al (100 nm) [device C:**tBuCN-FIroz**, device D:**tBuCN-FIrim**]. Device structure and the energy level diagram of vapor deposition and solution-process are given in Fig. S10 (ESI[†]).

Here, we used gradient hole injection layer (GraHIL) instead of the conventional PEDOT:PSS (AI 4083), as the former has merits of tuning the surface work function by self-organization, therefore, can effectively reduce the energy barrier for injection of holes into the EML. We incorporated a self-organized GraHIL composed of PEDOT:PSS and a perfluorinated polymeric acid, tetrafluoroethyleneperfluoro-3,6-dioxa-4-methyl-7-octene-sulfonic acid copolymer (PFI), with a low surface energy in 4:1 weight ratio, respectively. This ratios of GraHIL offers work function of ~ 5.6 eV, which is higher than PEDOT:PSS (~ 5.2 eV) [32,33]. Furthermore, PFI can shield the EML surface from the detrimental degradation by the acidic PEDOT:PSS. A mixed host containing tris(4-carbazoyl-9-ylphenyl)amine (TCTA) as the hole transporting and 2,6-bis(3-(carbazol-9-yl)phenyl)pyridine (DCzPPy) as the electron transporting material was optimized to a 4:6 ratio, respectively, for better confinement of excitons in EML. The optimal dopant ratio was 10 wt% similar to the dry process.

The J-V-L and the EQE-L characteristics of the PhOLEDs are given in Fig. 8a and b. The maximum EQEs of the PhOLEDs with **tBuCN-FIroz** and **tBuCN-FIrim** are 15.5% and 19.8%,

respectively. Here, EQE of **tBuCN-FIrim** based device is comparable to the EQE obtained in the vapor deposition process. Even though the EQE of **tBuCN-FIroz** based solution-processed device is a little lower than the corresponding vapor deposition result, the overall EQE is maintained moderately high. The T_1 energy level of **tBuCN-FIroz** ($T_1=2.66$ eV) has a very small energy difference with TCTA ($T_1=2.78$ eV) and DCzPPy ($T_1=2.71$ eV) compared to **tBuCN-FIrim** ($T_1=2.58$ eV). This might have caused poor energy transfer from the mixed host to the guest in case of **tBuCN-FIroz**, even though the V_{on} (4.5 eV) and current densities are similar for both the PhOLEDs. Moreover, we analysed the surface morphology and film formation of the EML of the two devices using the following configuration: ITO/GraHIL/EML by atomic force microscopy (AFM) (Fig. S11, ESI[†]). The root mean square (RMS) roughness of the EML surface for **tBuCN-FIroz** and **tBuCN-FIrim** are 1.12 and 0.93 nm, respectively. From this, it is obvious that the N-ethyl group in the ancillary ligand of **tBuCN-FIrim** has enhanced the solubility and film formation during spin-coating. As shown in Fig. 8c, the EL_{max} are slightly (4-6 nm) red shifted in both the PhOLEDs as compared to the solution PL spectra resulting in the CIE coordinates (0.152, 0.406) for **tBuCN-FIroz** and (0.215, 0.561) for **tBuCN-FIrim** at 10 mA cm^{-2} . These coordinates are almost unchanged even at 30 mA cm^{-2} . Results of the PhOLEDs fabricated in vapor deposition and solution process are given Table 2.

4. Conclusion

We designed and synthesized two Ir(III) complexes **tBuCN-FIroz** and **tBuCN-FIrim** with high PLQYs, excellent thermal and morphological stabilities, and good solubility in common organic solvents. Experimental observation of the photophysical process revealed that emission of **tBuCN-FIroz** and **tBuCN-FIrim** originates from the ancillary ligand centered excited state ($^3L_{AC}$) with substantial mixing of MLCT nature, by harvesting the excited state energy of both

C^N and ancillary ligands via ILET from C^N ligand to the low energy chromophoric ancillary ligand. The oxazoline and/or imidazoline heterocycle in the ancillary ligand not only enriched the MLCT contribution but also improved the rigidity of **tBuCN-FIroz** and **tBuCN-FIrim**. The substituents on C^N ligand (fluoro & cyano) have an effect of increasing intersystem crossings evidently from its (free C^N ligand) strong phosphorescence even in dilute solutions at low temperature as a representation of strong SOC. The monochromatic PhOLEDs fabricated with **tBuCN-FIroz** and **tBuCN-FIrim** as dopants via both solution-process and vapor deposition methods have resulted in the high efficiencies. Especially by vapor deposition process, the high EQE of 21.9% for **tBuCN-FIroz** with sky-blue CIE coordinates (0.149, 0.349) and 19.7% for **tBuCN-FIrim** with bluish-green coordinates (0.214, 0.504) were obtained. The PhOLED with **tBuCN-FIroz** exhibited a very minute roll-off in efficiency with EQE of 20.1% at 1000 cd m⁻².

Acknowledgments

This work was supported by grant fund from the National Research Foundation (NRF) (2011–0028320) and the Pioneer Research Center Program through the NRF (2013M3C1A3065522) by the Ministry of Science, ICT & Future Planning (MSIP) of Korea. This work (2014R1A2A1A01002030) was supported by Mid-career Researcher Program through NRF (National Research Foundation) grant funded by the MSIP (Ministry of Science, ICT and Future Planning).

References

- (1) Thierry S, Tondelier D, Declairieux C, Geffroy B, Jeannin O, Métivier R, et al. 4-Pyridyl-9,9'-spirobifluorenes as Host Materials for Green and Sky-Blue Phosphorescent OLEDs. *J. Phys. Chem. C* 2015;119:5790-5.

- (2) Lee SJ, Park JS, Yoon KJ, Kim Y-I, Jin S-H, Kang SK, et al. High-Efficiency Deep-Blue Light-Emitting Diodes Based on Phenylquinoline/Carbazole-Based Compounds. *Adv. Funct. Mater* 2008;18:3922–30.
- (3) Mukherjee S, Thilagar P. Recent advances in purely organic phosphorescent materials. *Chem. Commun* 2015;51:10988-1003.
- (4) Lee YH, Park J, Jo S-J, Kim M, Lee J, Lee SU, et al. Manipulation of Phosphorescence Efficiency of Cyclometalated Iridium Complexes by Substituted o-Carboranes. *Chem. Eur. J* 2015;21:2052-61.
- (5) Xu Q-L, Liang X, Zhang S, Jing Y-M, Liu X, Lu G-Z, et al. Efficient OLEDs with low efficiency roll-off using iridium complexes possessing good electron mobility. *J. Mater. Chem. C* 2015;3:3694-701.
- (6) Liu D, Ren H, Deng L, Zhang T. Synthesis and Electrophosphorescence of Iridium Complexes Containing Benzothiazole-Based Ligands. *ACS Appl. Mater. Interfaces* 2013; 5:4937-44.
- (7) You Y, Park SY. Phosphorescent iridium(III) complexes: toward high phosphorescence quantum efficiency through ligand control. *Dalton Trans* 2009:1267-82.
- (8) You Y, Seo J, Kim SH, Kim KS, Ahn TK, Kim D, et al. Highly Phosphorescent Iridium Complexes with Chromophoric 2-(2-Hydroxyphenyl)oxazole-Based Ancillary Ligands: Interligand Energy-Harvesting Phosphorescence. *Inorg. Chem* 2008;47:1476-87.
- (9) Chao K, Shao K, Peng T, Zhu D, Wang Y, Liu Y, et al. New oxazoline- and thiazoline-containing heteroleptic iridium(III) complexes for highly-efficient phosphorescent organic light-emitting devices (PhOLEDs): colour tuning by varying the electroluminescence bandwidth. *J. Mater. Chem. C* 2013;1:6800–6.

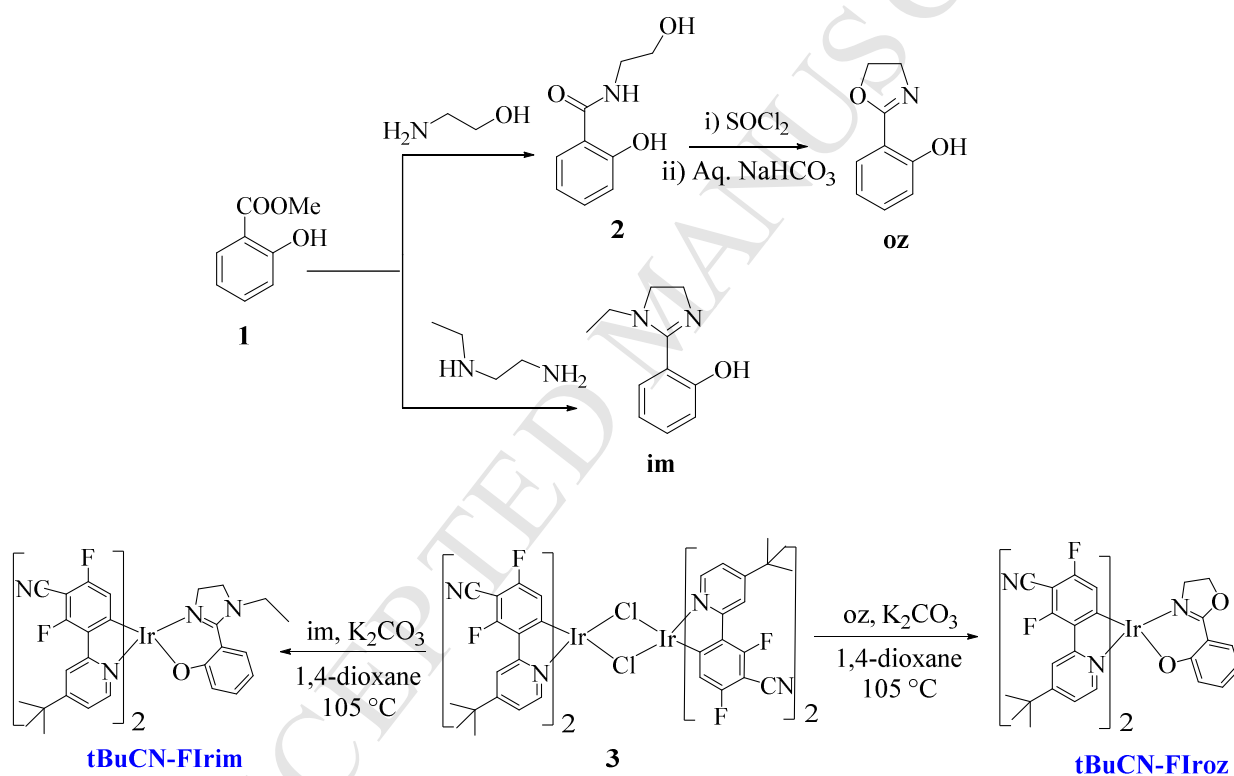
- (10) Si Y, Zhang S, Gahungu G, Yang J, Wu Z. Modification of the emission colour and quantum efficiency for oxazoline- and thiazoline-containing iridium complexes via different N[^]O ligands. *RSC Adv* 2015;5:18464-70.
- (11) Tong Y-P, Zheng S-L, Chen X-M. Syntheses, Structures, Photoluminescence, and Theoretical Studies of a Class of Beryllium(II) Compounds of Aromatic N,O-Chelate Ligands. *Inorg. Chem* 2005;44:4270-5.
- (12) Tao S, Lai SL, Yu J, Jiang Y, Zhou Y, Lee C-S, et al. Efficient Hole-Blocker with Electron Transporting Property and Its Applications in Blue Organic Light-Emitting Devices. *J. Phys. Chem. C* 2009;113:16792-5.
- (13) Yu G, Yin S, Liu Y, Shuai Z, Zhu D. Structures, Electronic States, and Electroluminescent Properties of a Zinc(II) 2-(2-Hydroxyphenyl)benzothiazolate Complex. *J. Am. Chem. Soc* 2003;125:14816-24.
- (14) Guillon H, Daniele S, Hubert-Pfalzgraf LG, Letoffe J.M. Synthesis, characterisation and thermal decomposition study of cerium(IV) 2-(2-hydroxyphenyl)-2-oxazoline derivatives. *Polyhedron* 2004;23:1467-72.
- (15) Sakai Y, Sagara Y, Nomura H, Nakamura N, Suzuki Y, Miyazaki H, et al. Zinc complexes exhibiting highly efficient thermally activated delayed fluorescence and their application to organic light-emitting diodes. *Chem. Commun* 2015;51:3181-4.
- (16) Oh CS, Lee JY. A thermally stable imidazole type ligand based Be complex as a triplet host material of green phosphorescent organic light emitting diodes. *Org. Electron* 2015;24:315-9.
- (17) Park S, Kwon JE, Kim SH, Seo J, Chung K, Park S-Y, et al. A White-Light-Emitting Molecule: Frustrated Energy Transfer between Constituent Emitting Centers. *J. Am.*

- Chem. Soc 2009;131:14043–9.
- (18) Qu X, Liu Y, Si Y, Wu X, Wu Z. A theoretical study on supramolecularly-caged positively charged iridium(III) 2-pyridyl azolate derivatives as blue emitters for light-emitting electrochemical cells. *Dalton Trans* 2014;43:1246–60.
- (19) Shang X, Han D, Zhan Q, Zhou D, Zhang G. Theoretical investigation of the effects of N-substitution on the photophysical properties of two series of iridium(III) complexes. *New J. Chem* 2015;39:2588-95.
- (20) Godefroid G, Juanjuan S, Xiaochun Q, Yuqi L, Yanling S, Xiaohong S. Shedding light on unusual photophysical properties of bis-cyclometalated iridium(III) complexes containing 2,5-diaryl-1,3,4-oxadiazole-based and acetylacetonate ligands. *Dalton Trans* 2012;41:10228-37.
- (21) Qu X, Liu Y, Godefroid G, Si Y, Shang X, Wu X, et al. Theoretical Study on Cationic Iridium(III) Complexes with a Diphosphane Ligand-Geometry, Electronic Properties, and Application for Light-Emitting Electrochemical Cells. *Eur. J. Inorg. Chem* 2013:3370–83.
- (22) Shang X, Li Y, Zhan Q, Zhang G. Theoretical investigation on the photophysical properties of a series of iridium(III) complexes with different substituted 2,5-diphenyl-1,3,4-oxadiazole. *New J. Chem* 2016:DOI: 10.1039/C5NJ02708J.
- (23) Yersin H, Finkenzeller WJ. Highly Efficient OLEDs with Phosphorescent Materials, Triplet Emitters for Organic Light-Emitting Diodes: Basic Properties; WILEY-VCH Verlag GmbH & Co. KGaA: Weinheim, 2008.
- (24) Luo Y, Xu Y, Zhang W, Li W, Li M, He R, et al. Theoretical Insights into the Phosphorescence Quantum Yields of Cyclometalated (C[∧]C^{*}) Platinum(II) NHC Complexes: π -Conjugation Controls the Radiative and Nonradiative Decay Processes. *J.*

- Phys. Chem. C 2016;DOI: 10.1021/acs.jpcc.5b12214.
- (25) Lustoň J, Kronek J, Böhme F. Synthesis and Polymerization Reactions of Cyclic Imino Ethers. I. Ring-Opening Homopolyaddition of AB-Type Hydroxyphenyl-Substituted 2-Oxazolines. *J. Polym. Sci., Part A: Polym. Chem* **2006**;44:343-55.
- (26) Lee J-H, Sarada G, Moon C-K, Cho W, Kim K-H, Park YG, et al. Finely Tuned Blue Iridium Complexes with Varying Horizontal Emission Dipole Ratios and Quantum Yields for Phosphorescent Organic Light-Emitting Diodes. *Adv. Opt. Mater* 2015;3:211-20.
- (27) Walmsley RS, Tshentu ZR, Fernandes MA, Frost CL. Synthesis, characterization and anti-diabetic effect of bis[(1-R-imidazolyl)phenolato]oxovanadium(IV) complexes. *Inorg. Chim. Acta* 2010;363:2215-21.
- (28) Sun C-Y, Wang X-L, Zhang X, Qin C, Li P, Su Z-M, et al. Efficient and tunable white-light emission of metal-organic frameworks by iridium-complex encapsulation. *Nat. Commun* 2013;4:2717, DOI: 10.1038/ncomms3717.
- (29) Zhang J, Zhao C, Liu H, Lv Y, Liu R, Zhang S, et al. Solvatochromic Fluorescence Emission of an Anthranol Derivative without Typical Donor-Acceptor Structure: An Experimental and Theoretical Study. *J. Phys. Chem. C* 2015;119:2761-9.
- (30) Pina J, de Melo J.S, Breusov D, Scherf U. Donor-acceptor-donor thienyl/bithienyl-benzothiadiazole/ quinoxaline model oligomers: experimental and theoretical studies. *Phys. Chem. Chem. Phys.* 2013;15:15204-13.
- (31) Kim K-H, Moon C-K, Lee J-H, Kim S-Y, Kim J-J. Highly Efficient Organic Light-Emitting Diodes with Phosphorescent Emitters Having High Quantum Yield and Horizontal Orientation of Transition Dipole Moments. *Adv. Mater* 2014;26:3844-7.
- (32) Han T.H, Song W, Lee T-W. Elucidating the Crucial Role of Hole Injection Layer in

Degradation of Organic Light-Emitting Diodes. ACS Appl. Mater. Interfaces 2015;7:3117-25.

- (33) Giridhar T, Han T-H, Cho W, Saravanan C, Lee T-W, Jin S-H. An Easy Route to Red Emitting Homoleptic Ir^{III} Complex for Highly Efficient Solution-Processed Phosphorescent Organic Light Emitting Diodes. Chem. Eur. J 2014;20:8260-4.



Scheme 1. Synthetic route of **tBuCN-FIroz** and **tBuCN-FIrim**.

FIGURE CAPTIONS

Fig. 1. ORTEP representation of **tBuCN-FIroz** (left) and **tBuCN-FIrim** (right). [Hydrogen atoms are omitted for clarity]

Fig. 2. (a) TGA curves; (b, c) DTA curves of the Ir(III) complexes at a heating rate of $10\text{ }^{\circ}\text{C min}^{-1}$ under N_2 atmosphere.

Fig. 3. (a) UV-Visible absorption & PL spectra in CHCl_3 (10^{-5} M), and neat film PL of the Ir(III) complexes; (b) PL spectra of the free ligands along with the Ir(III) complexes; (c, d) Representation of energy transfer from C^N ligand to the ancillary ligands. (RT=room temperature, f=film).

Fig. 4. Measurements of the excited state S_1 & T_1 energy levels from the PL study at room temperature (RT) and 77K (2-Me THF).

Fig. 5. Schematic representation of the photophysical process involved in **tBuCN-FIroz** and **tBuCN-FIrim**.

Fig. 6. DFT calculated HOMO-LUMO orbital distribution of **tBuCN-FIroz** and **tBuCN-FIrim**. [Hydrogen atoms were omitted for clarity]

Fig. 7. (a) $J-V-L$ characteristics; (b) $EQE-L$ characteristics; (c) EL versus PL; (d) CIE coordinates of the optimized PhOLEDs in vapor deposition process.

Fig. 8. (a) $J-V-L$ characteristics; (b) $EQE-L$ characteristics; (c) EL versus PL of the optimized PhOLEDs in solution-process.

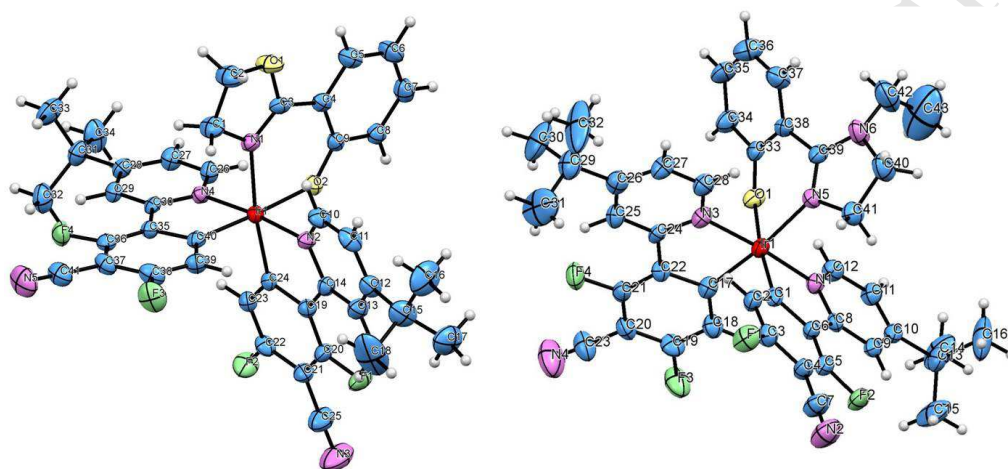


Fig. 1.

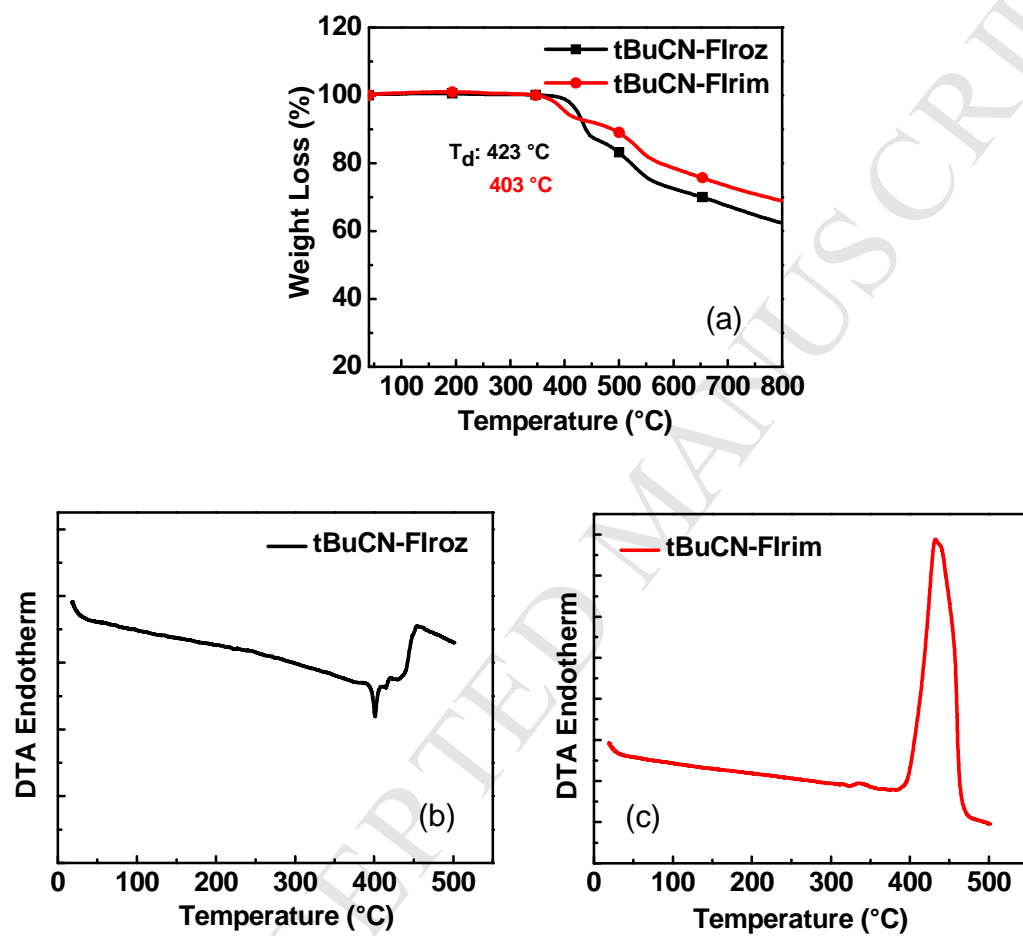


Fig. 2.

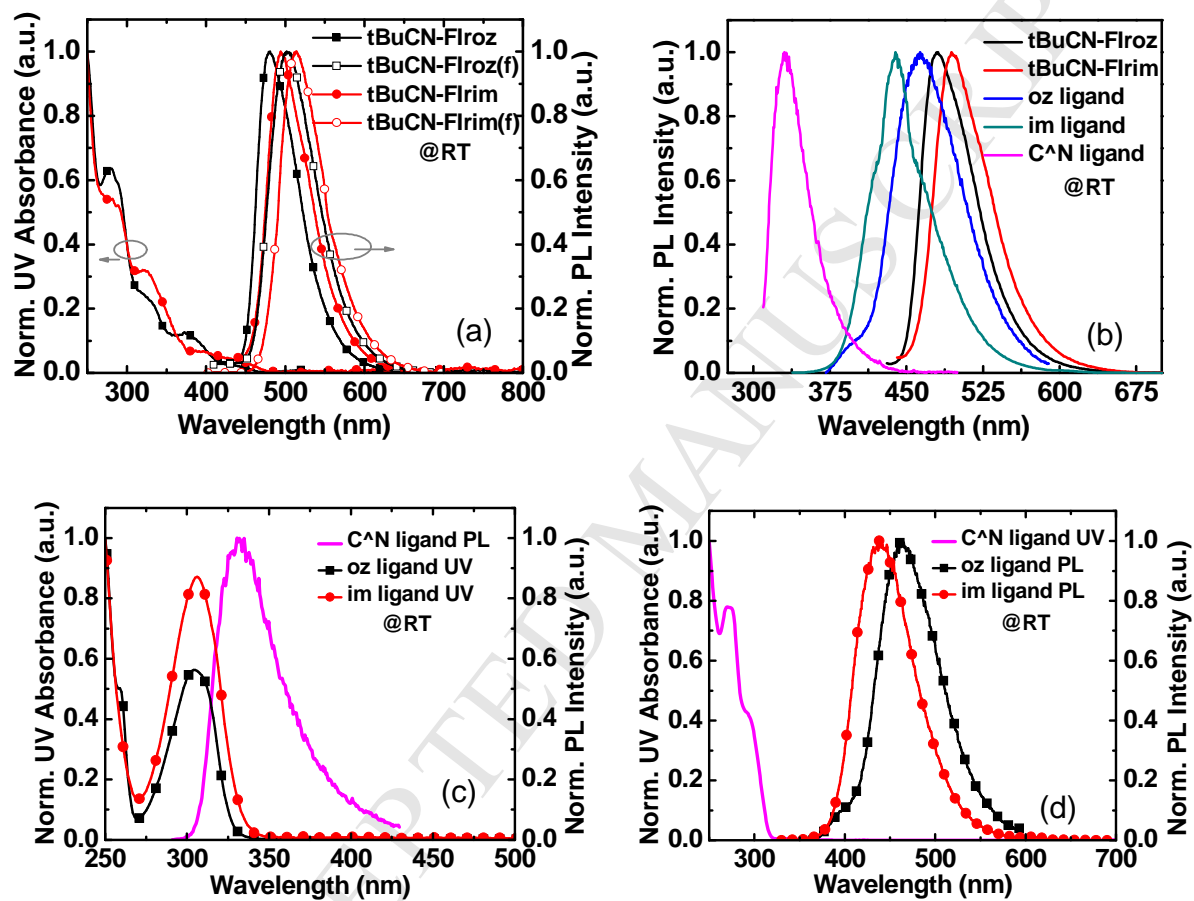


Fig. 3.

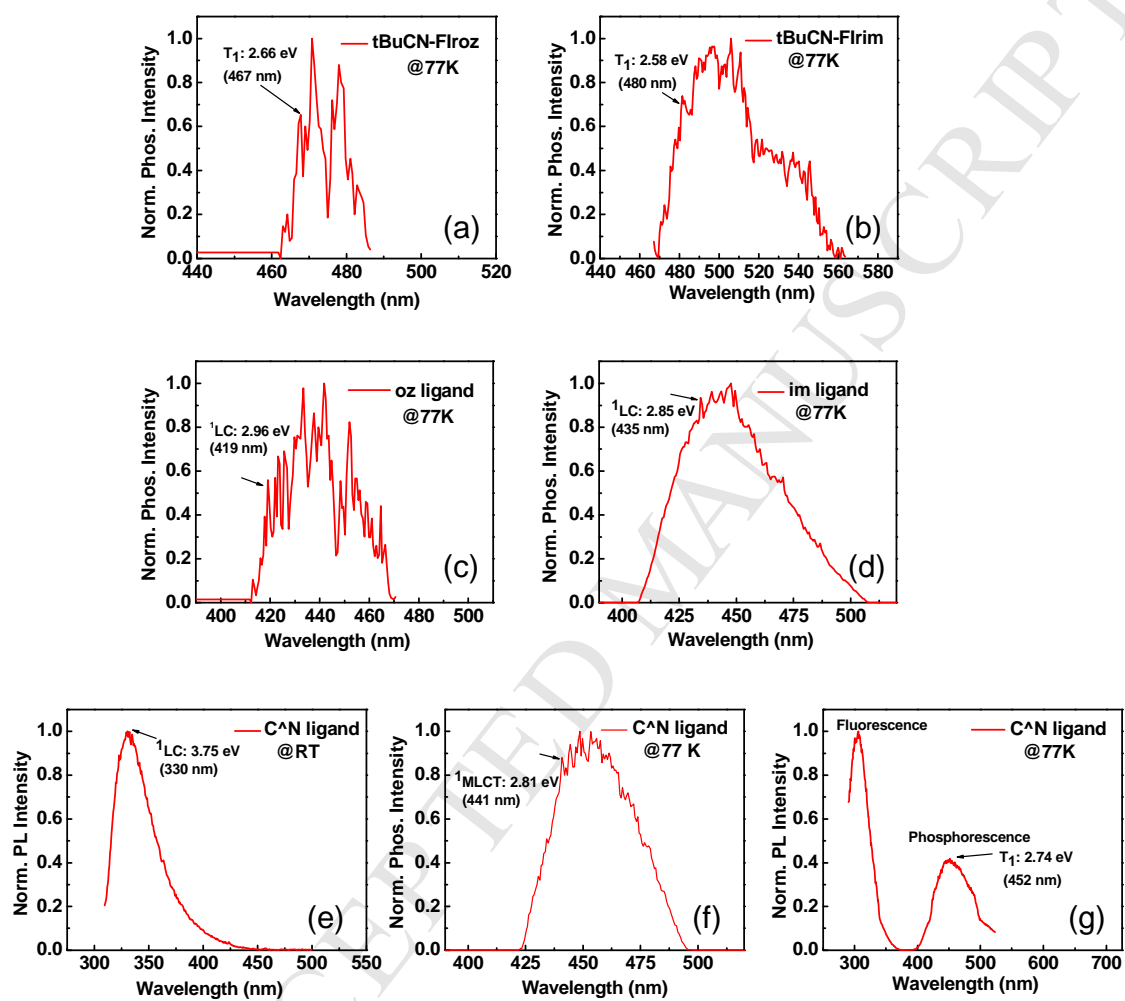


Fig. 4.

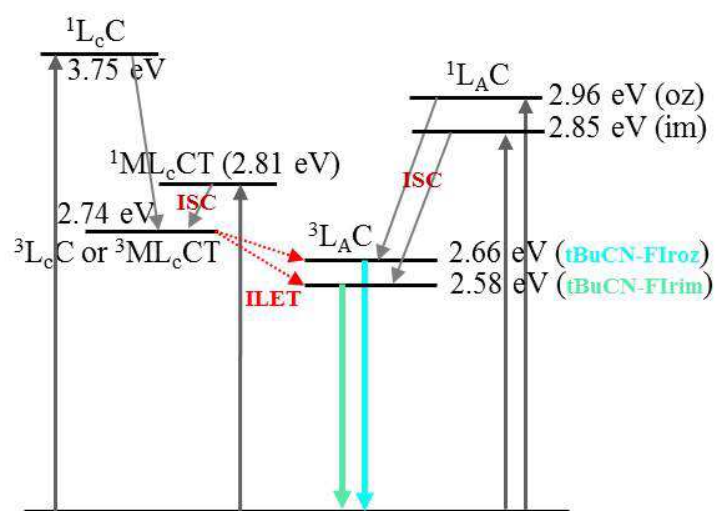


Fig. 5.

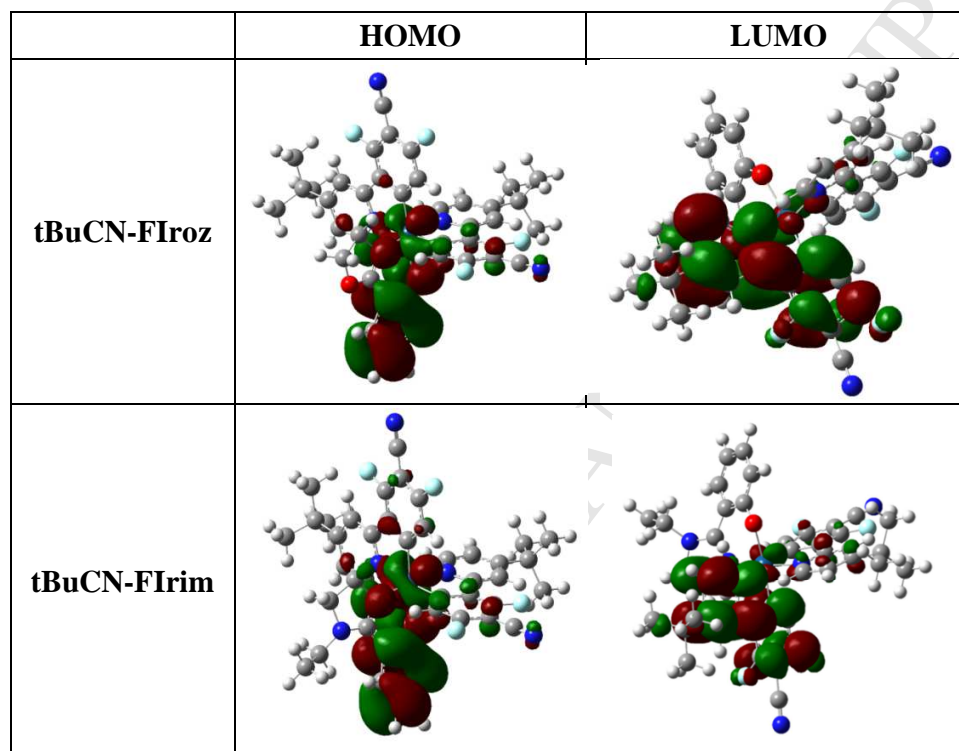


Fig. 6.

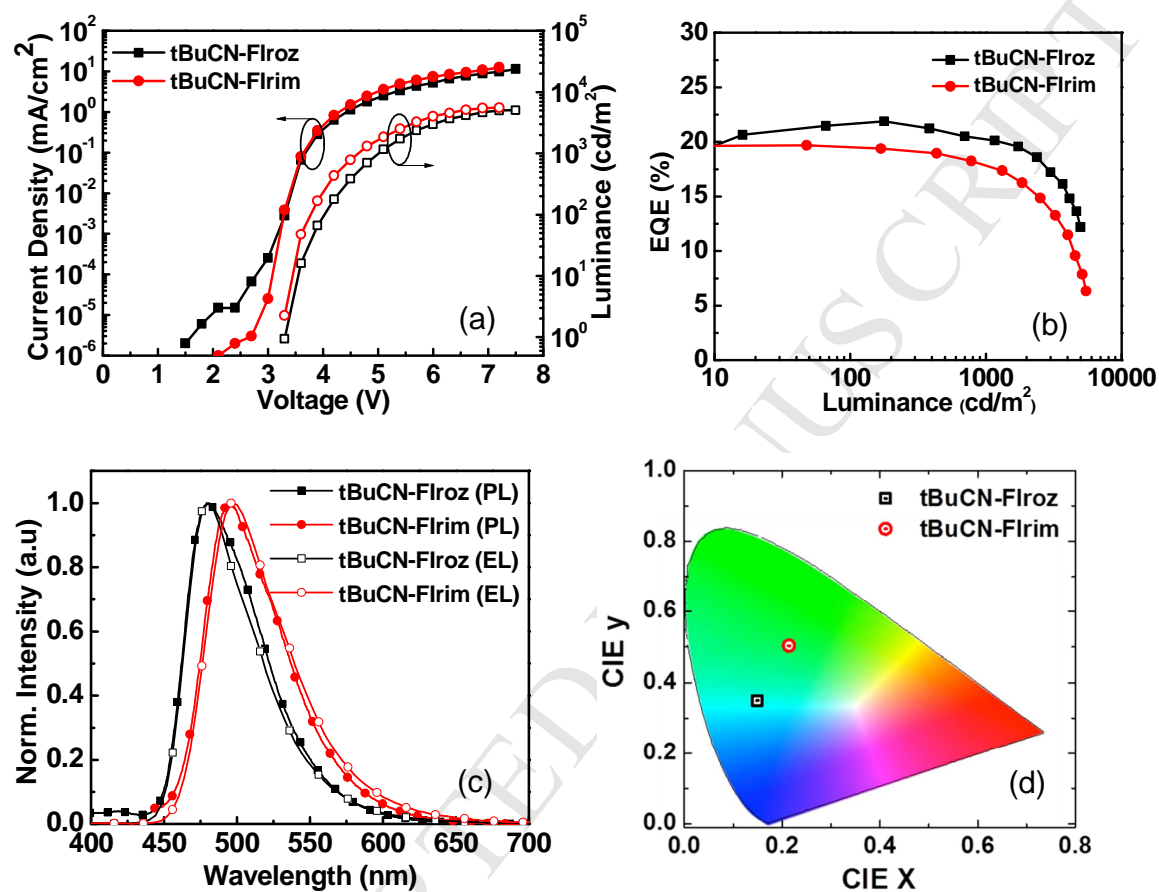


Fig. 7.

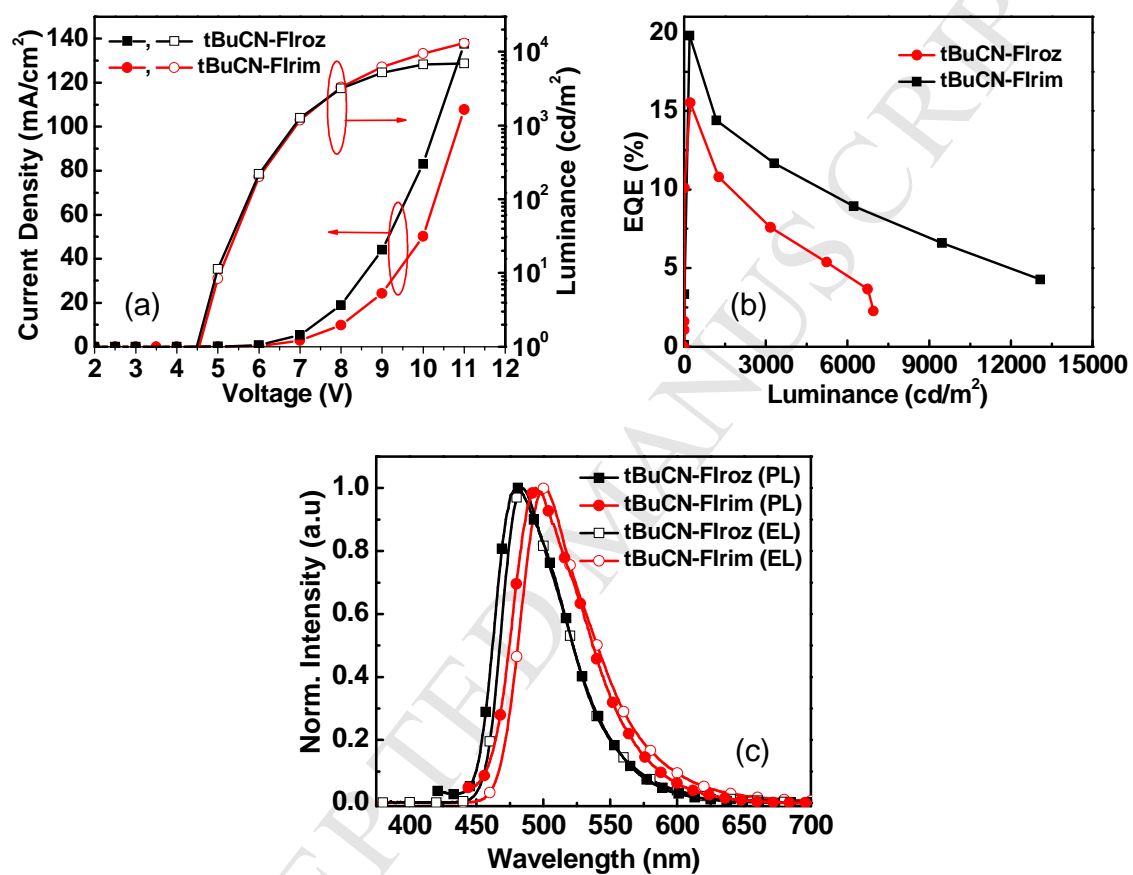


Fig. 8.

Table 1 Thermal, photophysical, and electronic properties of the Ir(III) complexes

	T_d	λ_{abs}	λ_{PL}	Φ_{pl}	Θ_H	μ	E_g	HOMO	LUMO
Complex	[°C]	[nm] ^{a,h}	[nm] ^a	[%] ^b	[%] ^c	[D] ^d	[eV] ^e	[eV] ^f	[eV] ^g
tBuCN-FIroz	423	280 (0.106), 326 (0.038), 373 (0.02)	480	90±3	78	12.04	2.73	-5.55	-2.82
tBuCN-FIrim	403	281 (0.061), 323 (0.035), 396 (0.006)	495	89±3	73	13.23	2.66	-5.50	-2.84

^a Measured in CHCl₃ solution at room temperature (10⁻⁵ M). ^b PLQYs of the thin films composed of pBCb2Cz:TSPO1:10% Ir(III) complexes measured on the quartz substrate. ^c Horizontal dipole ratio. ^d Permanent dipole moment. ^e Optical band gap. ^f Calculated from oxidation peak potentials from CV. ^g Calculated from HOMO and E_g. ^h ϵ values ($\times 10^5 \text{ M}^{-1} \text{ cm}^{-1}$) are shown in parentheses.

Table 2 EL characteristics of the monochromatic PhOLEDs with the new Ir(III) complexes

Device	V_{on}^a (V)	Maximum Device Performance at 1000 cd m^{-2}						EL_{max} (nm)	CIE ^c (x, y)
		EQE	PE	LE	EQE	PE	LE		
		(%)	(lm W^{-1})	(cd A^{-1})	(%)	(lm W^{-1})	(cd A^{-1})		
A (tBuCN-FIroz)	3.3	21.9	38.0	50.8	20.1	28.9	47.0	480 ^c	(0.149, 0.349)
B (tBuCN-FIrim)	3.3	19.7	48.0	55.0	17.4	50.8	35.4	496 ^c	(0.214, 0.504)
C (tBuCN-FIroz)	4.5	15.5	18.1	34.5	12.1	5.7 ^b	14.6 ^b	484 ^b	(0.152, 0.406)
D (tBuCN-FIrim)	4.5	19.8	30.1	57.5	15.4	8.4 ^b	24.2 ^b	501 ^b	(0.215, 0.561)

^a Turn on voltage at brightness of 1 cd m^{-2} . ^b Values collected at a current density of 30 mA cm^{-2} . ^c Values collected at a current density of 10 mA cm^{-2} .

Highlights

- Two Ir(III) complexes emitting a sky-blue and a bluish-green were synthesized.
- High photoluminescence quantum yield (PLQY~ 90%) was achieved.
- Chromophoric ancillary ligand and the –F/–CN groups play key role for high PLQY.
- PhOLEDs of these complexes show high performance in wet- and dry- processes.